Zhao *et al. Cell Communication and Signaling* (2024) 22:453
https://doi.org/10.1186/s12964-024-01823-3

Cell Communication and Signaling

RESEARCH Open Access

Histone variant H2AZ1 drives lung cancer progression through the RELA-HIF1A-EGFR signaling pathway

Huijie Zhao[1,2], Xing Wu[1], Yinghan Wang[1], Xiuling Li[2], Yuhui Du[1], Zhiqing Zhou[1], Yu Li[1], Yue Liu[1], Xiaofei Zeng[1,3] and Guoan Chen[1,4*]

Abstract

Background A growing body of evidence indicates that histone variants play an oncogenic role in cancer progression. However, the role and mechanism of histone variant H2AZ1 in lung cancer remain poorly understood. In this study, we aim to identify novel functions and molecular mechanisms of H2AZ1 in lung cancer.

Methods We analyzed H2AZ1 expression in lung adenocarcinoma using several RNA-seq and microarray datasets. Immunohistochemistry staining for H2AZ1 was performed on two sets of lung cancer tissue microarrays. To study the function of H2AZ1, we conducted assays for cell proliferation, colony formation, invasion, and migration. We employed CUT&Tag-seq, ATAC-seq, RNA-seq, and Western blotting to explore the regulatory patterns and potential mechanisms of H2AZ1 in lung adenocarcinoma.

Results Our findings reveal that H2AZ1 is highly expressed in lung cancer and high levels of H2AZ1 mRNA are associated with poor patient survival. Silencing H2AZ1 impaired cell proliferation, colony formation, migration, and invasion. Mechanistically, our CUT&Tag-seq, ATAC-seq, and RNA-seq results showed that H2AZ1 is primarily deposited around TSS and affects multiple oncogenic signaling pathways. Importantly, we uncovered that H2AZ1 may drive lung cancer progression through the RELA-HIF1A-EGFR signaling pathway.

Conclusion H2AZ1 plays an oncogenic role via several cancer-related pathways, including the RELA-HIF1A-EGFR axis in lung cancer. Intervention targeting H2AZ1 and its related signaling genes may have translational potential for precision therapy.

Keywords Lung cancer, H2AZ1, RELA, HIF1A, EGFR

*Correspondence:
Guoan Chen
cheng@sustech.edu.cn
[1]Department of Human Cell Biology and Genetics, Joint Laboratory of Guangdong-Hong Kong Universities for Vascular Homeostasis and Diseases, School of Medicine, Southern University of Science and Technology, No. 1088, Xueyuan Road, Nanshan District, Shenzhen, Guangdong Province 518055, China
[2]Department of Oncology, Sun Yat-sen Memorial Hospital, Sun Yat-sen University, Guangzhou, China
[3]National Key Laboratory for Tropical Crop Breeding, Shenzhen Branch, Guangdong Laboratory for Lingnan Modern Agriculture, Genome Analysis Laboratory of the Ministry of Agriculture, Agricultural Genomics Institute at Shenzhen, Chinese Academy of Agricultural Sciences, Shenzhen 518120, Guangdong, China
[4]The First Affiliated Hospital of Southern University of Science and Technology, Shenzhen, China

Background

Lung cancer is one of the most prevalent malignant tumors worldwide, ranking first in mortality and second in morbidity [1–3]. Early treatment can lead to a relatively good prognosis for most patients; however, once metastasis occurs (usually at stage III or IV), the disease can progress rapidly [4]. Unfortunately, effective treatments for advanced stages are lacking due to the unclear mechanisms of cancer progression and metastasis. This creates a bottleneck in improving treatment and underscores the need to deepen our understanding of the mechanisms behind lung cancer progression.

Histones are proteins rich in lysine and arginine residues, localized in the eukaryotic nucleus where they entwine and compress DNA to form chromatin. There are four main histone families: H1, H2, H3, and H4, each with distinct variants. The feature of histone families is the histone variants [5–7]. In mammalian cells, there are 11 variants of H1, 13 variants of H2, 8 variants of H3, and only 2 variants of H4 [6, 7]. These histone variants possess unique properties and modifications, adding complexity to chromatin structure. They regulate key developmental processes and, when dysregulated, may promote cancer development. A growing body of evidence indicates that histone variants are strongly linked to cancer and play a significant role in its progression [8–13]. The major variants of H2A include macro H2A, H2A.X, H2A.Bdb (B, L, P), and H2A.Z [6]. H2A.Z has two family members, H2AZ1 and H2AZ2, which differ by only three amino acids [14]. H2AZ1 has been reported to play vital roles in transcriptional regulation, DNA replication, and repair [6, 8, 15–17]. Nucleosomes containing H2AZ1 are classified as homotypic nucleosomes (containing two H2AZ1 proteins) and heterotypic nucleosomes (containing one H2AZ1 and one H2A protein), with homotypic nucleosomes being more stable due to the presence of acidic patches [18]. Heterotypic nucleosomes reduce nucleosome stability because the C-terminal sequence makes it easier for two H2A to interact [19]. The ability of H2AZ1 to reduce nucleosome stability is consistent with the pattern of H2AZ1 deposition in the enhancer and promoter regions: i.e., H2AZ1 is specifically deposited in the +1 nucleosome region, which is more likely to have a nucleosome-free region than other regions and is more likely to contain H2AZ1 and H3.3 nucleosomes. This may facilitate transcription factor binding [20]. It has been reported that H2AZ1 promotes and represses transcription, likely by affecting nucleosome positioning. The absence of H2AZ1 results in unclear nucleosome positioning in key promoter regions, while the addition of H2AZ1 leads to nucleosome repositioning. If the new position hinders the accessibility of positive regulatory sequences, H2AZ1 binding will repress transcription, and if the new position increases the accessibility of positive regulatory sequences, it will enhance transcription [21]. The specific role and mechanisms played by H2AZ1 in the regulation of gene transcription still require more comprehensive and precise studies.

There is increasing focus on the role of H2AZ1 in various tumors [9, 10, 22]. In breast cancer, MYC binds to the promoter region of H2AZ1 and recruits H2AZ1 under estrogen-stimulated conditions. High H2AZ1 expression indicates a poor prognosis for breast cancer [23]. H2AZ1 is present on a subset of active enhancers bound by estrogen receptor α (ER) and these enhancers produce enhancer RNAs (eRNAs) and recruit RNA polymerase II as well as RAD21, which are involved in chromatin interactions between enhancers and promoters [24]. In prostate cancer, acetylated H2AZ1 in the enhancer region increases chromatin accessibility and expression of ectopic genes [25]. However, comprehensive studies on the role and molecular mechanisms of H2AZ1 in lung cancer progression are rare [26, 27].

In this study, we found that H2AZ1 is highly expressed in lung cancer, and the high level of H2AZ1 mRNA expression is associated with poor survival in lung cancer patients. Silencing H2AZ1 impaired cell proliferation, migration, and invasion. Mechanistically, our CUT&Tag-seq (Cleavage Under Targets and Tagmentation sequencing), ATAC-seq (Assay for Transposase Accessible Chromatin with high-throughput sequencing), and RNA-seq experiments revealed the regulatory pattern of H2AZ1 and its modulation of crucial cancer-related signaling pathways in lung cancer. Importantly, we discovered that H2AZ1 may drive lung cancer progression through the RELA-HIF1A-EGFR signaling pathway, suggesting intervention with H2AZ1 and its related signaling genes may have potential clinical relevance for cancer therapy.

Methods

Cell lines and culture

Lung cancer cell lines H838, A549, H1299, PC9, and H1975 were used to carry out the experiments, all the cell lines were purchased from the Cell Bank of the Chinese Academy of Sciences (Shanghai, China). The cell lines were cultured with the medium that contained RPMI 1640 (Gibco), 10% fetal bovine serum (Gibco), and 1% penicillin-streptomycin (Gibco). The culture conditions of cells were proper humidity, 37℃, and 5% CO2. We observed the cells every day, passaged at 80% confluent, and collected the cells in the logarithmic growth phase to conduct the subsequent study. To confirm cell line identity, genotyping was performed at Guangzhou Cellcook Biotech CO., Ltd.

siRNA-mediated knockdown

SiRNAs and negative control siRNA were purchased from GenePharma (Suzhou, China). H838, A549, H1299, PC9, and H1975 cells were collected and plated in six-well plates at 0.8–1.2×10^5 cells/well. After 24 h, the cells were transfected with siRNA using RNA Lipofectamine RNAi max (Invitrogen, USA) in six-well plates, following the manufacturer's protocol. At 48 h after transfection, the cells were collected to perform function experiments and RNA extraction. Protein extraction was performed at 72 h after transfection. H2AZ1 siRNA target sequences are listed in the Supplementary Table S1.

Construct stable cell lines with lentiviral vector

A lentiviral vector LV10N(U6/mCherry&Puro) (Gene Pharma) was used to construct short hairpin (sh) RNA for H2AZ1. A lentiviral vector GV492 (Genechem Co., LTD., Shanghai, China) was used to construct stable cell lines to overexpress H2AZ1. The oligos-specific sequence is listed in Supplementary Table S1.

Cell proliferation assay

Cell proliferation was determined with a Cell Counting Kit (CCK8) (Yeasen, Shanghai, China). Cells were collected and diluted, seeded in 96-well plates (1000 cells/well), and 5 ~ 6 biological replicates were conducted in each group. The outer rows were filled with 100ul PBS to prevent liquid evaporation. After 24 h, H2AZ1 siRNA was used to transfect the cells. Then, 10ul CCK8 was added to each well at 72 h after transfection and the plates were incubated for 1 h. The Optical density (OD) 450 values were used to evaluate the cell viability.

Colony formation assay

Cells were collected at 48 h after H2AZ1 siRNAs transfection, then seeded in 6-well plates at 500 cells/well and cultured for 10 ~ 14 days. When the cell count was equal to or greater than 50 in one clone, the cells were washed with PBS, fixed with methanol, and stained with 1% crystal violet. Image J software was used for colony counting. Percentage of colony formation (%) = colony number/500×100%.

Transwell assay for cell migration and invasion

Cell invasion experiments were conducted in 8.0-μm Falcon Cell Culture Inserts (Corning, USA, REF 353097). Matrigel Basement Membrane Matrix (Corning, USA, REF 356234) was dissolved at 4℃ and diluted (1:8) with cold RPMI1640 medium. 100 μL diluted matrigel was added to the upper chamber and cultured for 4 ~ 5 h in a cell incubator. 2 ~ 4×10^4 cells were suspended in 200 ~ 400 μl RPMI1640 medium and placed in the upper chamber. The lower chamber was filled with 600 μl medium with 10% FBS. After incubation for 24 ~ 48 h, the cells were fixed with methanol and stained with crystal violet. The pictures (4x, and 10x) were taken after cleaning the bottom of the upper chamber with cotton. The cell migration assay was conducted similarly to cell invasion experiments, except the inserts were not coated with Matrigel.

Western blotting

Western blotting was conducted to measure protein expressions. Cells grown in a 6 cm dish were washed twice with cold PBS and lysed with RIPA buffer (Cell Signaling Technology, USA, REF 9806 S) which contained 1% PMSF (Beyotime, Shanghai, China, REF ST506-2), and 1% Protease & phosphatase inhibitor (Thermo Fisher Scientific, USA, REF 1861280). The protein was collected and quantified by colorimetric protein assay (Thermo Fisher Scientific, USA, REF 23225). 20 μg proteins were loaded onto 4-20% or 4-12% SDS-PAGE gel (GenScript, Nanjing, China, M00654), then transferred to 0.2 μm PVDF membrane (Roche, Shanghai, China, REF 03010040001). The membrane was blocked with 5% BSA (Sigma-Aldrich, CAS: 9048468) for 2 h, incubated with primary antibodies (Cell Signaling Technology, USA, antibodies listed in Supplementary Table S1) overnight at 4 °C. The next day, the membranes were incubated with the secondary antibody (1:5000, Cell Signaling Technology, USA) at room temperature for 1 h. The result was detected with ChampChemi 610 plus, a fully automated chemiluminescence instrument (Sage creation, Beijing, China) after TBST (Boster, USA) washing three times.

RNA extraction and qRT-PCR

RNA extraction (Vazyme, Nanjing, China, RC112-01) and reverse transcription(Takara, Japan, RR047A) were performed following Kits instructions. The cDNA was diluted and used for qRT-PCR. qRT-PCR was performed with TB Green Premix EX Taq II (Takara, Japan, RR820L). GAPDH was used as the endogenous reference. Primers are listed in the Supplementary Table S1.

RNA-seq

Cells were grown in 6-cm dishes and transfected with siRNAs (H2AZ1 siRNAs and siCtrl) on the following day. 48 h after transfection, total RNA was extracted using triazole, and the concentration and purity of the extracted RNA were measured using Nanodrop 2000. The strand-specific library-building strategy was used to save the strand orientation information into the sequencing library. A flexible differential analysis strategy was used to obtain differentially expressed mRNAs. These were performed in GENE DENOVO (Guangzhou, China) and FRASERGEN (Wuhan, China).

ATAC-seq

Cells (H2AZ1 siRNAs and siCtrl treated) were collected, and then a lysis buffer was added to obtain the nucleus. DNA fragments were obtained by adding Tn5 transposes and then amplified and sequenced. These were performed in FRASERGEN (Wuhan, China), and the detailed experimental procedure was referenced to Corces MR [28] and Fujiwara S [29].

CUT&Tag-seq

CUT&Tag-seq was performed in FRASERGEN (Wuhan, China). In brief, cells were bound by concanavalin A-coated magnetic beads. After the cells were permeabilized by digitonin, the primary antibodies against the target protein (H2AZ1) were added, followed by the incubation of secondary antibodies, and then pAG-conjugated transposase enzyme (pAG-Tn5) was added to bind the antibodies, with the activation of Tn5 by Mg2+. The DNA fragments close to the target protein were cut and thereby detached from chromatin. Oligomer-tagged fragments were extracted, screened for those less than 700 bp, amplified, and sequenced. These were performed in FRASERGEN (Wuhan, China) and the detailed experimental procedures can be found in Kaya-Okur's report [30].

Immunohistochemistry of tissue array

Lung cancer tissue arrays (TMAs) were purchased from Shanghai Outdo Biotech Company (Cat No. HLug-A180Su08, Shanghai, China). For immunohistochemical (IHC) staining on TMAs, the slices were dried at 63 °C for 1 h. Then, the slides were dewaxed in xylene and dehydrated in ethanol. Antigen repair was performed by microwave in sodium citrate. 3% hydrogen peroxide was used to block endogenous peroxidase. After washing off the hydrogen peroxide, 10% goat serum was used to block it for half an hour. The primary antibody was incubated at 37 °C for 1 h, and the secondary antibody was incubated for 15 min (primary and secondary antibodies information were shown in Supplementary Table S1). The color was developed with a DAB detection system. Counterstaining was performed with hematoxylin.

Published microarray and RNA sequencing data collections

Three published microarray data sets of lung cancer were downloaded. These included Okayama et al., 226 LUADs (lung adenocarcinoma) with stage 1 and 2 [31], Shedden et al., with 442 stage 1 to 3 LUADs [32] and Hou et al., with 45 LUAD, 19 LCC (large cell carcinoma), 27 SCC (squamous cell cancer), and 65 normal lung tissues [33]. The original CEL files of microarray data were normalized using the Robust Multi-array Average (RMA) method [34]. We also obtained two RNA-seq data sets including Seo et al., with 78 LUAD and 77 normal lung tissues [35], TCGA data with 309 LUAD, 212 SCC, and 73 normal lung tissues [36]. Expression levels of transcripts were represented as FPKM [37].

Statistical analysis

Two-sided Student's t-tests were performed for the comparison between different groups, with $p<0.05$ as a criterion for statistical significance. Kaplan-Meier survival curve with log-rank test was used for survival analysis. GO and KEGG enrichment analysis of selected genes from RNA-seq, CUT&Tag, and ATAC-seq data were performed using the DAVID website (https://david.ncifcrf.gov/), Correlation analysis using the GEPIA website (http://gepia.cancer-pku.cn/). RNA-seq, CUT&Tag, and ATAC-seq read were aligned to human reference genome hg38, Ensembl-release100. IGV (The Integrative Genomics Viewer) [38] was used for the visual exploration of genomic data.

Results

H2AZ1 is highly expressed in lung cancer and associated with poor patient survival

In Boire's study on a brain metastasis mouse model of lung cancer [39], Lewis lung cancer cells were injected into the left ventricle and the medulla oblongata pool of the cerebellum in mice, successfully establishing brain parenchymal and meningeal metastasis models after three cycles. The primary Lewis lung cancer cells (Parental), and the cells of intermediate generation metastatic (Inter), meningeal metastatic (Leptom), and brain parenchymal metastatic (BrM) were collected and RNA-seq was performed. Our re-analysis of these RNA-seq data revealed that the histone variant *H2az1*(*H2afz*) was highly expressed in mouse lung cancer brain parenchymal metastases (Fig. 1A, B). Additionally, in a gene expression profile study by Kikuchi's group on metastatic brain tumors from lung adenocarcinomas, *H2AZ1* was among the top highly expressed genes in metastatic brain tumors compared to primary lung adenocarcinomas [40]. H2AZ1 has been reported to be overexpressed in metastatic melanoma compared to primary melanoma [12].

We analyzed H2AZ1 expression across various clinical lung cancer datasets to explore its relationship with clinical and pathological characteristics. Analysis of mRNA gene microarray data from 91 non-small cell lung cancers and 65 paraneoplastic tissues from Hou [33] revealed that *H2AZ1* mRNA was highly expressed in lung adenocarcinoma, large cell carcinoma, and squamous lung cancer tissues (Fig. 1C). Similar findings were observed in RNA-seq data from Seo in Korea [35] and TCGA in the USA [36], where *H2AZ1* was also highly expressed in lung cancer tissues (Fig. 1D, E). The Shedden dataset [32], comprising mRNA microarray data from 442 lung adenocarcinoma tissues with clinical and pathological

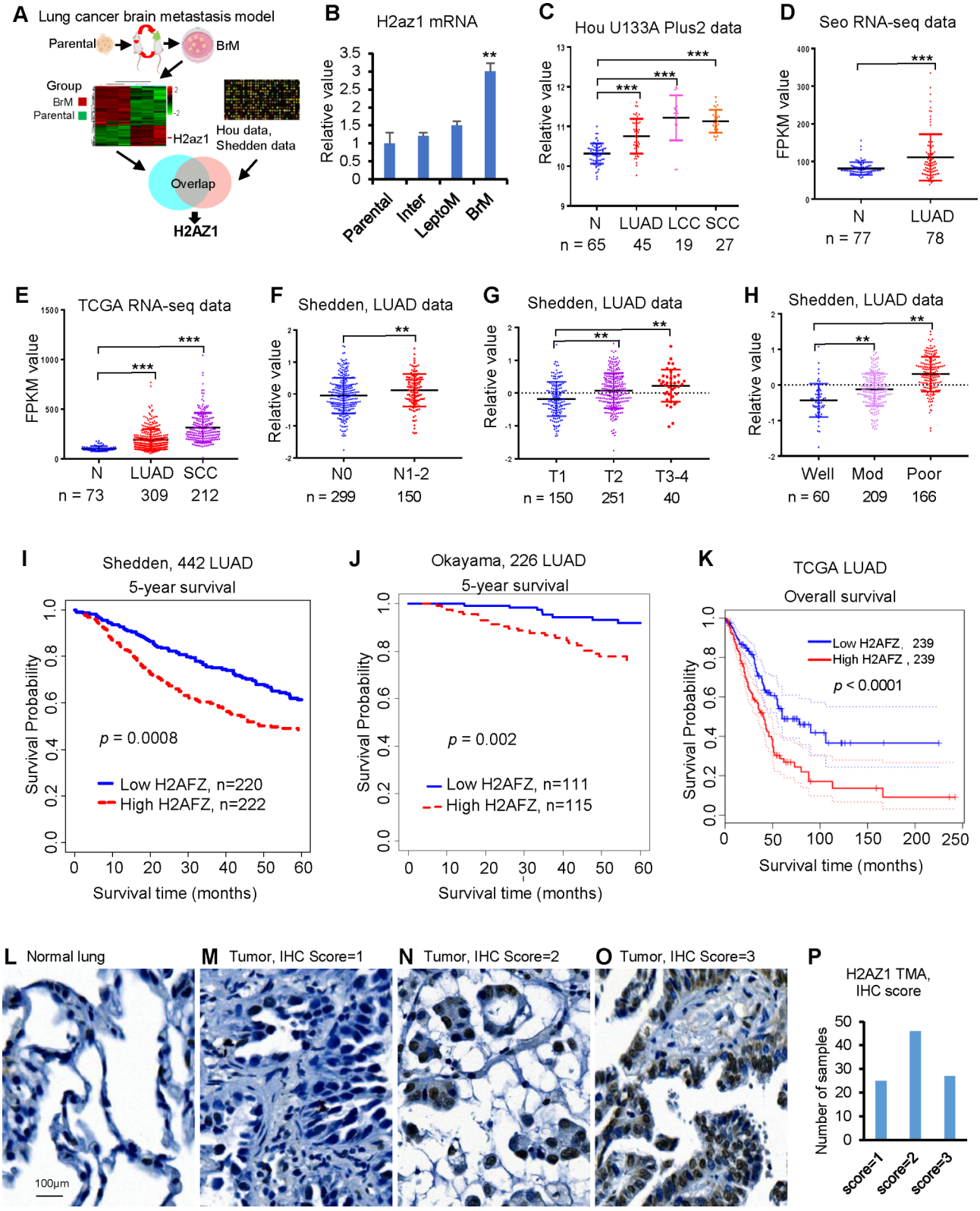

Fig. 1 (See legend on next page.)

(See figure on previous page.)

Fig. 1 H2AZ1 is highly expressed in non-small cell lung cancer and a high level of H2AZ1 is associated with poor patient survival in lung cancer. (**A**) The flow of screening the target gene, H2AZ1, based on public databases. On the left are the mouse metastatic model and gene profile, and right is the human lung cancer gene expression profile. (**B**) The expression of *H2az1* mRNA at different sites and stages in the mouse model. Parental: parental Lewis cells, Inter: intermediate cells, Leptom: cells collected from meninges metastases, BrM: cells collected from brain parenchymal metastases. (**C**) In Hou's microarray data, as compared to normal lung tissues (**N**), *H2AZ1* mRNA was highly expressed in lung adenocarcinoma (LUAD), large cell cancer (LCC)and squamous cell carcinoma (SCC), *** $p < 0.001$. (**D**, **E**) In Seo and TCGA RNA-seq data, *H2AZ1* mRNA was highly expressed in LUAD and SCC, *** $p < 0.001$. (**F**-**H**) In Shedden microarray data, *H2AZ1* mRNA expression was significantly increased in lymph node metastasized, large tumor size, and poorly differentiated tumors, ** $p < 0.01$. (**I** -**K**) Kaplan-Meier survival analysis showed that a high level of *H2AZ1* mRNA was associated with poor survival in patients with lung cancer in 3 LUAD data sets. (**L**-**P**) Representative microphotographs of H2AZ1 IHC on lung TMA. Weak staining signal of H2AZ1 in normal tissues and some tumor tissues (Score = 1); Moderate staining signal of H2AZ1 in some tumor tissues (Score = 2); Strong staining signal of H2AZ1 in some tumor tissues (Score = 3). The distribution number of each score from TMA180 is shown in P

information, showed significantly higher *H2AZ1* mRNA expression in lymph node metastases, large tumors, and poorly differentiated tumors (Fig. 1F-H).

Survival analysis of the Shedden dataset indicated that high *H2AZ1* mRNA level was associated with poor patient survival (Fig. 1I). This correlation was further supported by Okayama data [31], which is a gene microarray data from early-stage (stage 1 and 2) lung adenocarcinoma tissues (Fig. 1J), and TCGA RNA-seq data from the GEPIA website of lung adenocarcinoma (LUAD) (Fig. 1K).

To investigate H2AZ1 protein expression in lung cancer tissues, we performed immunohistochemistry (IHC) staining of H2AZ1 on two lung cancer tissue microarrays (TMAs). One TMA includes 180 cores with 98 lung adenocarcinomas and para-cancerous lung tissues, while the other TMA includes 150 cores with 75 lung adenocarcinomas and para-cancerous lung tissues (Fig. S1A, B). Most tumors showed strong H2AZ1 protein staining with a score of 2 or 3 (Fig. 1L-P). IHC on three pairs of primary lung carcinomas and brain metastatic tumors from lung cancer also showed strong H2AZ1 protein staining (Fig. S1C-F).

To explore *H2AZ1* mRNA expression status in other types of cancer, we performed the normal vs. tumor and survival analysis based on the GEPIA website [41]. Our findings revealed that *H2AZ1* mRNA was highly expressed in several cancers, including adrenocortical carcinoma, colon adenocarcinoma, liver hepatocellular carcinoma, and skin cutaneous melanoma, and the higher expression level was correlated with poor patient survival in these cancers (Fig. S1G, H). These results indicate that high H2AZ1 expression is not limited to lung cancer but is also prevalent in multiple other cancer types. Collectively, H2AZ1 is highly expressed in multiple cancers, and its higher expression was correlated to poor patient survival in several cancers including lung cancer. This suggests that H2AZ1 could serve as a valuable biomarker for cancer diagnosis and prognosis. The increased expression of H2AZ1 in both primary and metastatic tumors indicates its potential role as an oncogenic gene involved in cancer progression, warranting further studies on its oncogenic functions and molecular mechanisms in cancer.

H2AZ1 silencing impairs cell proliferation, colony formation, migration, and invasion in lung cancer

To explore the oncogenic function of H2AZ1, we first tested the knockdown efficiency and specificity of siRNAs targeting H2AZ1 using qRT-PCR, Western blot, and RNA-seq. Results showed that both H2AZ1 mRNA and protein levels were decreased by more than 90% after H2AZ1 siRNAs treatment in four lung cancer cell lines (Fig. 2A, B).

Next, we investigated the oncogenic function of H2AZ1 in vitro using cell proliferation, colony formation, migration, and invasion assays. The results showed that the cell proliferation and colony formation were significantly decreased after H2AZ1 silencing with siRNAs in 4 lung cancer cell lines (Fig. 2C-E), suggesting H2AZ1 could promote tumor cell growth. The cell migration and invasion capacity were impaired upon H2AZ1 knockdown (Fig. 2F-I), indicating H2AZ1's role in promoting tumor cell metastasis.

To confirm these findings, we overexpressed H2AZ1 in H1299 and A549 cell lines, which increased colony formation (Fig. S2A-D). Collectively, H2AZ1 knockdown impaired cell proliferation, colony formation, migration, and invasion, suggesting H2AZ1 plays an oncogenic role in lung cancer progression. Next, we conducted CUT&Tag-seq, ATAC-seq, and RNA-seq experiments in three lung cancer cell lines (H1975, A549, and H1299) to explore the molecular mechanisms of H2AZ1 in lung cancer progression from multiple omics perspectives.

H2AZ1 binding to TSS causes higher gene expression and affects multiple cancer-related signaling pathways revealed by CUT&Tag and RNA-seq

To uncover the relationship between the H2AZ1 chromatin deposition pattern and gene expression profile, we performed the CUT&Tag-seq with an H2AZ1 antibody and RNA-seq after the H2AZ1 silencing with siRNAs. Although the H2AZ1 binding density and number of peaks/genes varied among the three cell lines (Fig. 3A-E), H2AZ1 chromatin binding signals were strongly

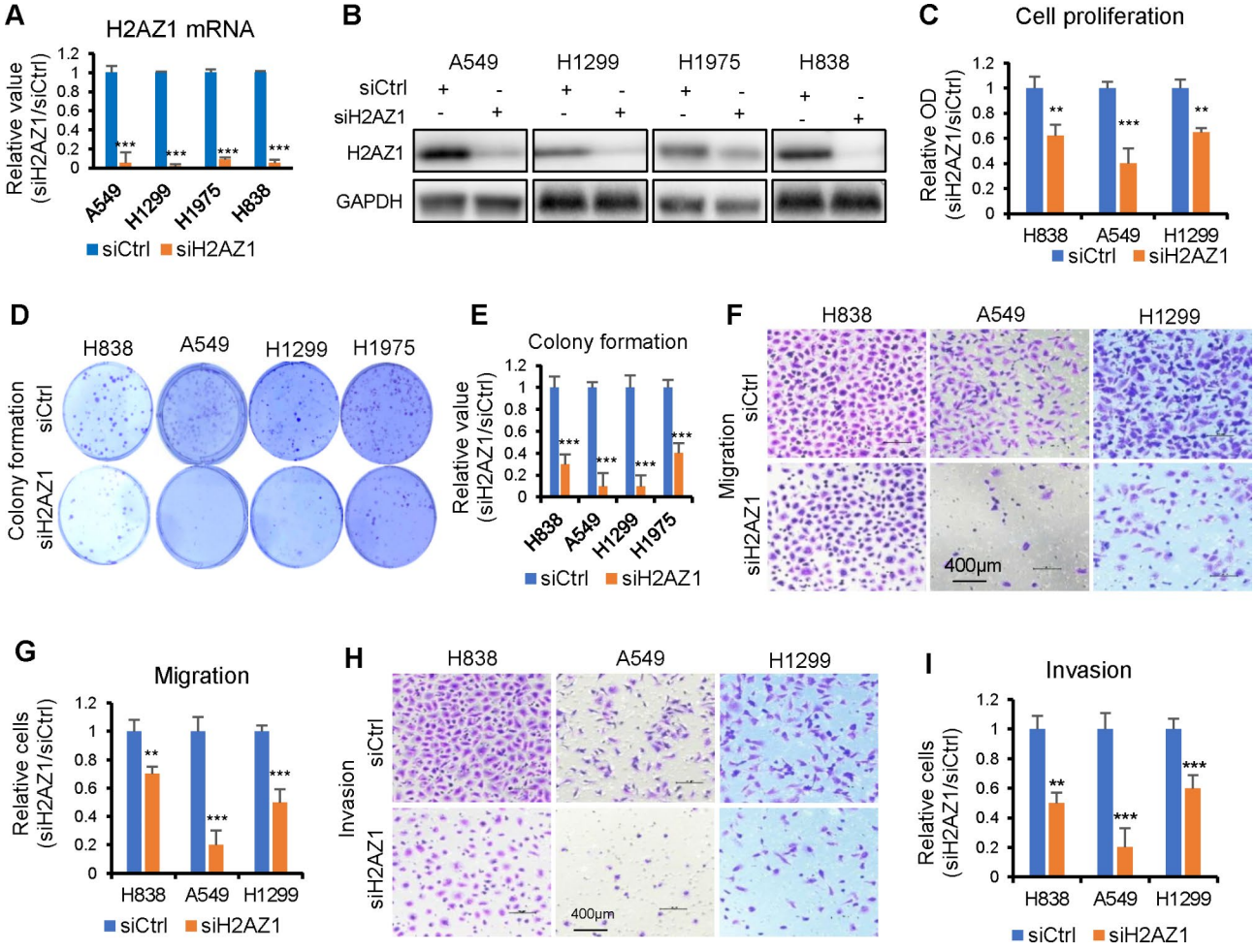

Fig. 2 H2AZ1 silencing impairs cell proliferation, colony formation, migration, and invasion. (**A**) qRT-PCR showing that *H2AZ1* mRNA was reduced after siRNA treatment at 48 h in lung cancer cells in A549, H1299, H1975, and H838 lung cancer cell lines. (**B**) Western blot showing that H2AZ1 protein was decreased after siRNA treatment at 72 h in lung cancer cells. (**C**) Cell proliferation was decreased after H2AZ1 knockdown by siRNAs in lung cancer cells, ** $p < 0.01$, *** $p < 0.001$. (**D**, **E**) Colony formation was decreased after H2AZ1 knockdown with siRNAs, *** $p < 0.001$ (**E** is the quantitative result for **D**). (**F-I**) Migration and invasion were decreased after H2AZ1 silencing with siRNAs in lung cancer cells (**G** was the quantitative result of **F**, **I** was the quantitative result of **H**), ** $p < 0.01$, *** $p < 0.001$

enriched around transcriptional start sites (TSS) (Fig. 3B, C), consistent with previous reports [42]. There was less H2AZ1 binding in the gene body (Fig. S3A). Interestingly, the distribution of H2AZ1 binding around TSS showed a low binding zone (0 region of TSS) possibly the RNA polymerase II and transcription factors binding region or H2AZ1 less deposited in 0 region (Fig. 3B-D). H2AZ1 binding peaks were mainly located at the promoter region within 1 kb (39.2-46.6%) in three cell lines (Fig. 3F). Further, we found that the H2AZ1 DNA binding peaks occupying the chromatin had commonality and heterogeneity in these three cell lines (Fig. 3G). Common H2AZ1 DNA binding peaks in the three cell lines were enriched mainly in the gene promoter region within 1 kb (77.5%) (Fig. 3H), while differential peaks were distributed in distal intergenic regions (35.1%), the 1st introns (14.1%) and other introns (25.7%) (Fig. 3I). Most importantly, gene enrichment of the common peaks in Fig. 3H shows that multiple important cancer-related signaling pathways were enriched including cell cycle, autophagy, MAPK, Hippo, mTOR, p53, ErbB, Wnt, and cell adhesion (Fig. 3J and S3B), which further confirmed important oncogenic roles of H2AZ1 shown in Figs. 1 and 2. Subsequent investigation of the molecular mechanisms of these pathways is warranted.

The correlation between the H2AZ1 chromatin binding intensity and location and transcriptional activity in lung cancer cells is not well understood. Based on RNA-seq value, we classified the genes into four classes according to their expression levels (based on siCtrl or siH2AZ1, respectively) and aligned them to CUT&Tag signals in the TSS and gene body regions. The results revealed that the higher H2AZ1 binding intensity in the promoter region around TSS positively correlated with higher gene

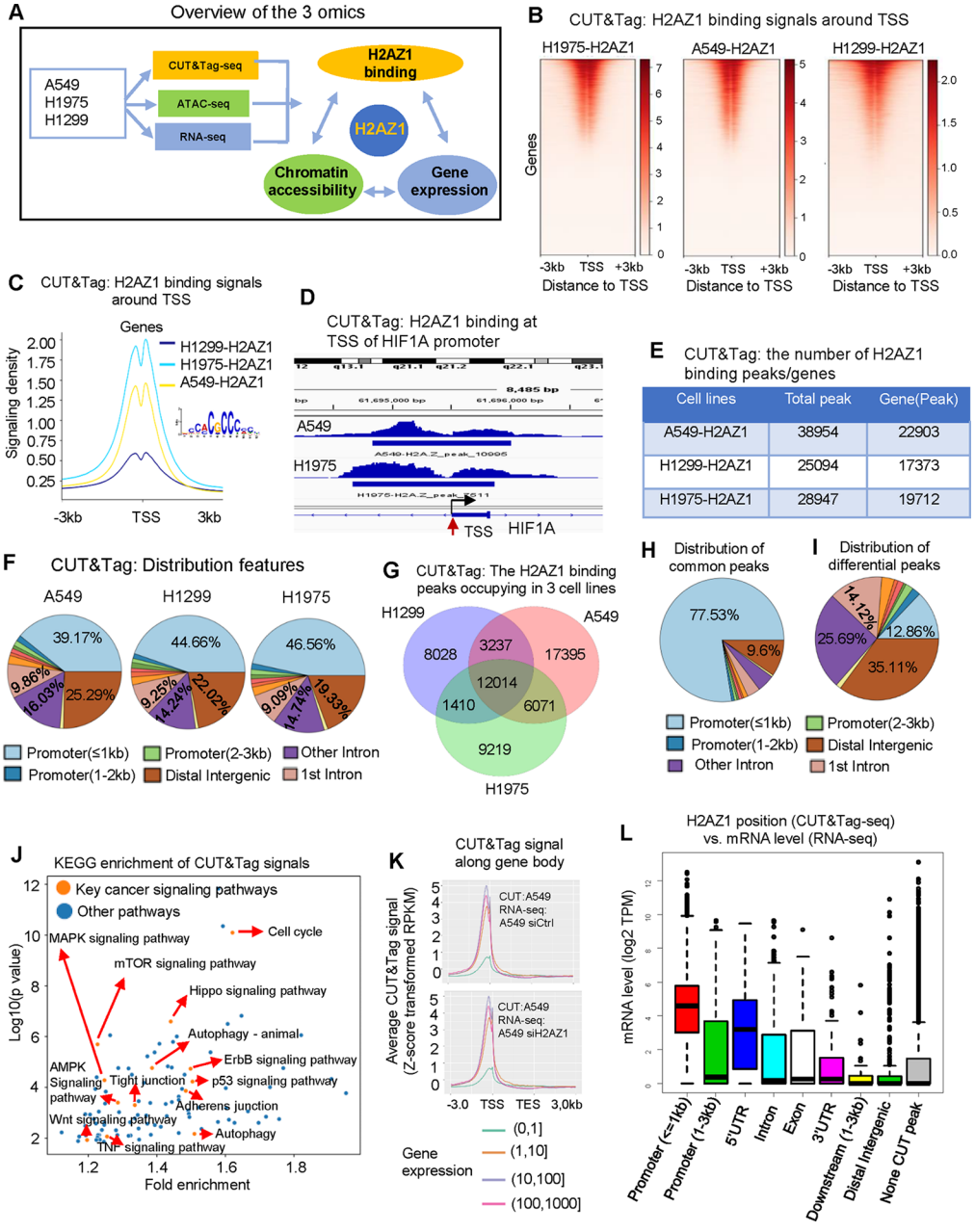

Fig. 3 H2AZ1 binding to TSS causes higher gene expression and affects multiple cancer-related signaling pathways revealed by CUT&Tag-seq and RNA-seq. (**A**) Overview of the CUT&Tag-seq, ATAC-seq, and RNA-seq experimental design. (**B**, **C**) CUT&Tag-seq revealed the distribution of H2AZ1 binding signals around TSS. H1299 had a relatively lower intensity. (**D**) A representative CUT&Tag image showing H2AZ1 binding at the TSS of HIF1A promoter, having two binding regions around the TSS. (**E**) CUT&Tag-seq: The number of H2AZ1 binding peaks and genes in the peaks in 3 lung cancer cell lines. (**F**) CUT&Tag-seq: Distribution of H2AZ1 binding peaks in the chromatin in 3 cell lines. (**G**) CUT&Tag-seq: The Venn diagram revealed the landscape overlap of H2AZ1 peaks occupying the chromatin in 3 lung cancer cell lines. (**H**) CUT&Tag-seq: round pie chart showing the distribution regions of the common peaks of the 3 cell lines. (**I**) CUT&Tag-seq: round pie chart showing the distribution regions of the differential peaks of the 3 cell lines. (**J**) KEGG enrichment of CUT&Tag-seq of the genes corresponding to the common peaks of 3 cell lines were significantly enriched in important cancer-related signaling pathways. (**K**) Correlation analysis of H2AZ1 binding density by CUT&Tag-seq and gene expression of RNA-seq data revealed the relationship between H2AZ1 binding (CUT&Tag signal) and gene expression (RNA-seq) in the A549 cell line. (**L**) The more detailed relationship between the location of H2AZ1 on chromatin deposition and gene expression. (H1975 of CUT&Tag and RNA-seq of H1975 siCtril as an example showing here, A549 and H1299 have similar results not shown here)

expression, while no such correlation was observed in the gene body region (Fig. 3K and S3C), consistent with previous reports [12, 42, 43].

We then investigated in more detail the correlation of gene expression levels and different locations of H2AZ1 on chromatin using CUT&Tag and RNA-seq data. The results revealed that most genes were bound to the promoter within less than 1 kb of TSS (Figs. S3D) and the gene expression levels were higher when H2AZ1 bound to the promoter (<=1 kb) and 5'UTR regions (Fig. 3L). Conversely, gene expression levels were much lower or not expressed when H2AZ1 bound to gene body regions (including promoter (1-3 kb), intron, exon, distal intergenic, downstream, and 3'UTR), or in regions without binding (Fig. 3L). This may be the reason why there was no correlation between H2AZ1 binding intensity and gene expression in the gene body region shown in Fig. 3K. Importantly, this relationship between H2AZ1 chromatin deposition and gene expression was validated in human lung tissues using TCGA RNA-seq data [36] which includes 73 normal lung tissue, 309 LUAD, and 212 LUSC (Fig. S3E-G) indicating that H2AZ1 promoter deposition is critical for gene expression.

Interestingly, combined analysis of H2AZ1 binding from CUT&Tag-seq and the differentially expressed genes from RNA-seq found a similar number of up or down-regulated genes in H2AZ1 binding regions (Fig. S3H), indicating that H2AZ1 binding on chromatin can cause both gene up-regulation and down-regulation, depending on other unknown mechanisms.

Collectively, our CUT&Tag and RNA-seq analyses show that H2AZ1 chromatin binding peaks are strongly enriched around TSS and that common peaks are involved in multiple cancer-related pathways. H2AZ1 binding intensity is positively correlated with gene expression levels only in the promoter region around TSS. Genes were expressed only when H2AZ1 binds to the promoter (<=1 kb) and 5'UTR regions, but not when it binds to other regions suggesting that H2AZ1 deposition on chromatin to the promoter (<=1 kb) and 5'UTR regions is critical for an active gene expression. Additionally, H2AZ1 binding on chromatin can lead to both up-regulation and down-regulation of gene expression upon H2AZ1 silencing.

Open chromatin accessibility at TSS leads to higher gene expression revealed by ATAC-seq and RNA-seq

To determine if chromatin accessibility was affected by H2AZ1, we performed ATAC-seq analysis after H2AZ1 knockdown with siRNAs and controls (siCtrl). The ATAC-seq peak signals enriched within +/-3 kb of TSS were similar across three cell lines (Fig. 4A, B and S4A), although the total number of peaks varied among these cell lines (Fig. 4C). The changes in peak number upon siH2AZ1 treatment have differed among cell lines. For instance, peak numbers decreased (from 63619 to 42905) in H1975, increased (from 84703 to 89287) in H1299, and unchanged in A549 cells (Fig. 4C). Chromatin accessibility was predominantly located at the promoter (<=1 kb) (21.6-39.3%), distal intergenic (20.1-24.7%), and other introns (17.1-25.3%), and these distributions did not change after H2AZ1 silencing (Fig. 4D and S4B). Chromatin accessibility exhibited both commonality and heterogeneity among the three cell lines (Fig. 4E), with common peaks primarily located in the gene promoter region within 1 kb (63%) (Fig. 4F), like CUT&Tag results shown in Fig. 3H.

We then analyzed the gain or loss of DAR (Differentially Accessible Region) upon H2AZ1 knockdown from ATAC-seq data and found that the number of the gain or loss of DAR varied among the cell lines (Fig, 4G). The number of genes in the gain or loss DAR was also different among the cell lines (Fig. 4H). In H1299 cells, there were 16,202 genes in the gain DAR, and 13,346 in the loss DAR. Conversely, in H1975 cells, there were 7,231 genes in the gain DAR and 16,510 genes in the loss DAR. In A549 cells, the number of genes in the gain or loss DAR was nearly equal to the siH2AZ1 treatment (Fig. 4H). This trend was also observed in the DAR-associated promoter genes across the three cell lines (Fig. S4C). These results suggest that H2AZ1 knockdown can cause both gain and loss DAR.

KEGG enrichment analysis of loss DAR promoter genes after H2AZ1 silencing demonstrated that the genes mainly enriched in tumor-related signaling pathways such as cell adhesion, Wnt, HIF1A, Hippo, and ErbB, etc. (Fig. S4D). Key genes in these pathways were also altered, such as EGFR and CCNE1, which will be validated in the subsequent experiments.

A high density of ATAC-seq signaling means that the chromatin regions are more open and more accessible for transcription factors and RNA polymerase binding, showing a correlation between chromatin accessibility near genes and their expression levels. We analyzed the relationship between gene expression levels and chromatin accessibility using ATAC-seq and RNA-seq data. We divided genes into four classes based on expression levels and aligned them to ATAC-seq signals in the TSS or gene body. We found that the ATAC-seq signal intensity in TSS was positively correlated with gene expression regardless of H2AZ1 knockdown, while no correlation was found in the gene body region (Fig. 4I and S4E). All six samples showed the same patterns, suggesting that genes with high expression levels usually had more open chromatin status only at the TSS region.

Further detail analysis indicated that gene expression levels were higher only if chromatin was open in the promoter (<=1 kb) region (Fig. 4J and S4F). In contrast, gene

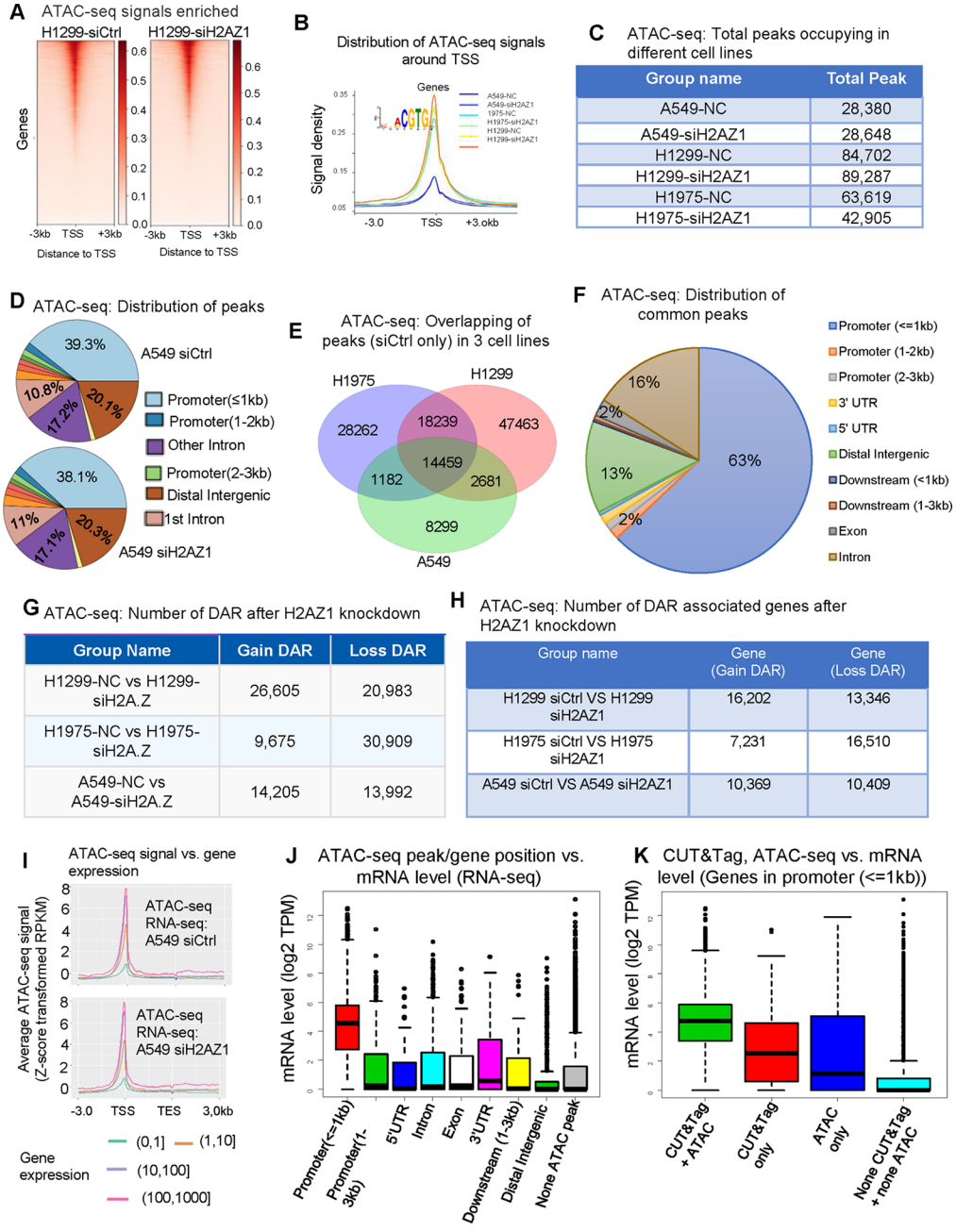

Fig. 4 Open chromatin accessibility at TSS leads to higher gene expression revealed by ATAC-seq and RNA-seq. (**A**, **B**) ATAC-seq signals density around TSS. A549 had a relatively lower intensity. (**C**) ATAC-seq revealed the total peaks with H2AZ1 silencing or not in 3 lung cancer cell lines. (**D**) Distribution of peaks on chromatin accessibility in A549 cell line. (**E**) Venn diagram of ATAC-seq showed the overlapping of chromatin accessibility of 3 lung cancer cell lines (siCtrl data only). (**F**) ATAC-seq: round pie chart showing the distribution of chromatin accessibility regions of the common peaks of the 3 cell lines (siCtrl data only). (**G**) The number of gain or loss DARs upon H2AZ1 silencing in 3 cell lines. (**H**) ATAC-seq shows the number of gain or loss DAR-associated genes after H2AZ1 knockdown. (**I**) The relationship between chromatin accessibility (ATAC-seq signal) and gene expression (RNA-seq) in the A549 cell line. (**J**) The more detailed relationship between chromatin accessibility and gene expression. (H1975 siCtrl of ATAC-seq and RNA-seq of H1975 siCtril as an example showing here, A549 and H1299 have similar results not shown here). (**K**) The correlation of H2AZ1 deposition, chromatin accessibility, and gene expression in the promoter (<=1 kb) CUT&Tag-seq, ATAC-seq, and RNA-seq data. (CUT&Tag-seq of H1975, ATAC-seq of H1975 siCtrl, and RNA-seq of H1975 siCtril as an example showing here, A549 and H1299 have similar results not shown here)

expression levels were very low or nonexistent if chromatin was open in gene body regions (including promoter (1-3 kb), intron, exon, distal intergenic, downstream, and 3'UTR), or in regions with no open chromatin (Fig. 4J). This explains why there was no correlation between ATAC signal intensity and gene expression in the gene body region shown in Fig. 4I. More importantly, this relationship between chromatin accessibility location

and gene expression was verified in human lung tissues from TCGA RNA-seq data [36] (Fig. S4H-J) indicating that opened chromatin at the promoter is a key factor for gene expression in both normal and tumor tissues.

From CUT&Tag-seq and ATAC-seq analysis, we concluded that genes were expressed only if H2AZ1 deposited, or chromatin opened only on the promoter (<=1 kb) region. Next, we analyzed the relationship between gene expression levels and H2AZ1 binding and/or chromatin accessibility in the promoter (<=1 kb) region. We found that the gene expression was higher when there was both H2AZ1 binding and open chromatin, compared to H2AZ1 binding only or open chromatin only (Fig. 4K and S4G). An example of the correlation among CUT&Tag, ATAC, and mRNA expression is shown in Fig. S4K, L. ING5, D2HGDH, and LINC01279 gene locations having H2AZ1 binding signaling (CUT&Tag) and open chromatin around TSS (ATAC-seq) have mRNA expression (RNA-seq), while NEU4, PDCD1 (PD1) and RTP5 gene locations having not H2AZ1 binding signaling and open chromatin around TSS have not mRNA expression in all 3 lung cancer cell lines. This relationship between H2AZ1 binding and/or chromatin accessibility in the promoter (<=1 kb), and gene expression was confirmed in lung tissues from TCGA RNA-seq data [36] (Fig. S4M-O).

In summary, common chromatin accessibility peaks were mainly distributed in the gene promoter region within 1 kb (63%) among the three cell lines. H2AZ1 knockdown could cause both gain DAR and loss DAR. Gene expression levels were positively correlated with higher chromatin accessibility signal only in the TSS region, and gene expression levels were higher only if chromatin opened in the promoter (<=1 kb) region. The highest gene expression level was related to H2AZ1 binding and chromatin accessibility in the promoter (<=1 kb) region in both normal and tumor tissues.

H2AZ1 is involved in multiple cancer-related signaling pathways uncovered by RNA-seq

To fully understand the regulation of H2AZ1 on gene expression, we performed RNA-seq after the knockdown of H2AZ1 with siRNAs in A549, H1299, and H975 cell lines. We used the following criteria for the selection of up or down-regulated genes upon H2AZ1 knockdown: (1) TPM value larger than 0.3 in 2/3 samples; (2) siH2AZ1/siCtrl ratio less than 0.65 or greater than 1.6 in 2 of 3 cell lines. We identified 908 down-regulated genes and 1026 up-regulated genes upon H2AZ1 knockdown in these three lung cancer cell lines (Fig. S5A). KEGG pathway enrichment analysis on the DAVID website [44] for these 908 down-regulated genes revealed the enrichment in several important cancer-related pathways, such as TNF, NF-kB, HIF1A, PD-L1/PD-1, MAPK, pathways in cancer, cell adhesion, JAK-STAT, and PI3K-AKT (Fig. 5A). These results were consistent with previous CUT&Tag enrichment results. Further analysis showed that several core genes related to lung cancer, including RELA, HIF1A, and EGFR, frequently appeared in these pathways (Fig. 5B, C). Interestingly, among the 908 down-regulated genes, 128 were transcription factors (TFs). KEGG pathway enrichment with these 128 TFs revealed a similar pathway pattern to that seen with all 908 genes (Fig. S5B). This warranted further investigation into how H2AZ1 regulates these oncogenic genes and pathways. Analysis of the 1026 up-regulated genes revealed that the herpes simplex virus 1 infection was among the top pathways, followed by renin and insulin resistance (Fig. S5C). Surprisingly, Key tumor suppressor genes [45], such as TP53, PTEN, RB1, STK11, NF1, and KEAP1did not change upon H2AZ1 knockdown as measured by RNA-seq (Fig. S5D).

In previous analyses of CUT&Tag, ATAC-seq, and RNA-seq data, several cancer-related signaling pathways were enriched, including key molecules in lung cancer such as RELA, HIF1A, and EGFR. We validated these findings at both protein and mRNA levels using Western blotting (Fig. 5D and S5E, F). The results demonstrated that the protein levels of EGFR, HIF1A, and p-RELA p65 were reduced after H2AZ1 knockdown (Fig. 5D). We confirmed that proteins of EGFR, HIF1-α, and p-RELA p65 were also decreased by stable knockdown H2AZ1 with shRNAs in A549 and PC9 cell lines (Fig. S5E, F), constant with RNA-seq results (Fig. 5C). These findings suggested that these oncogenic genes are regulated by H2AZ1 at the transcription level. We next investigated the relationship between these oncogenic genes and H2AZ1.

H2AZ1 regulates EGFR through HIF1A

HIF1A is reported to promote EGFR transcription through its binding to the 18th intron of the EGFR gene in breast cancer cells using ChIP-seq and double luciferase reporter assay [46]. We showed that H2AZ1 regulates HIF1A and EGFR at both mRNA and protein levels. Since HIF1A is a transcription factor that could regulate EGFR [46], we speculated that H2AZ1 may regulate EGFR through HIF1A by binding to the promotor regions of EGFR in lung cancer.

First, we confirmed that H2AZ1 regulates HIF1A. HIF1A was decreased upon H2AZ1 silencing (Fig. 5C, D and S5E, F). We then overexpressed H2AZ1 and HIF1A with lentivirus. HIF1A expression was upregulated after H2AZ1 overexpression (Fig. 6A), while H2AZ1 expression was slightly decreased after HIF1A overexpression, possibly as a feedback reaction (Fig. 6A). From TCGA RNA-seq data of human lung adenocarcinoma tissues on the GEPIA website [41], we found a strong positive correlation between H2AZ1 mRNA and HIF1A mRNA

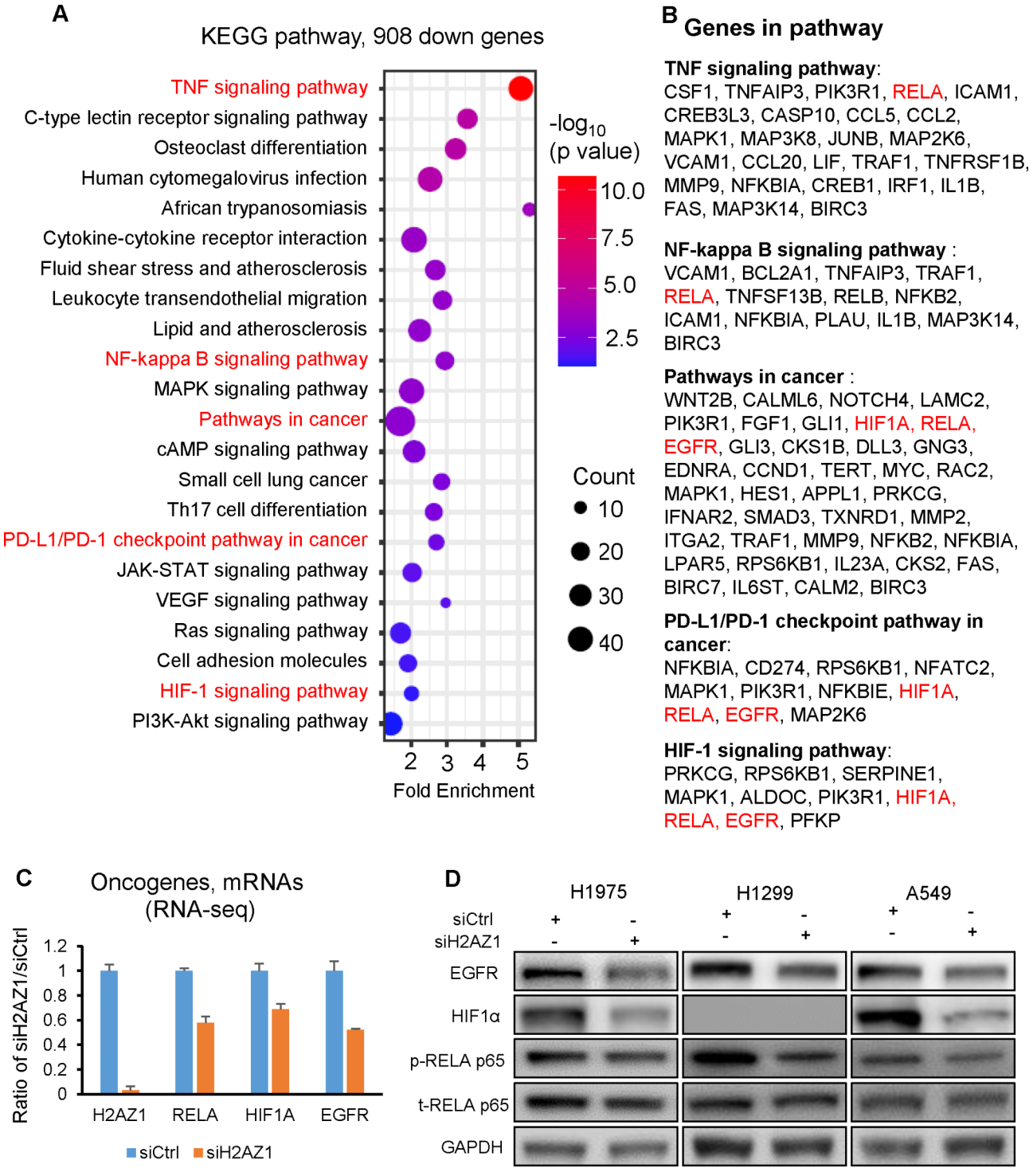

Fig. 5 H2AZ1 knockdown affects several cancer-related pathways. (**A**, **B**) KEGG pathway enrichments using 908 down-regulated genes after H2AZ1 knockdown. Several cancer-related pathways and oncogenic genes are highlighted in **B**. (C) RNA-seq data indicated that the mRNAs of RELA, HIF1A, and EGFR were reduced after H2AZ1 knockdown with siRNAs. (**D**) Western blot demonstrated that the protein levels of EGFR, HIF1αand RELA p65 were decreased after H2AZ1 knockdown with siRNAs at 72 h in 3 lung adenocarcinoma cell lines

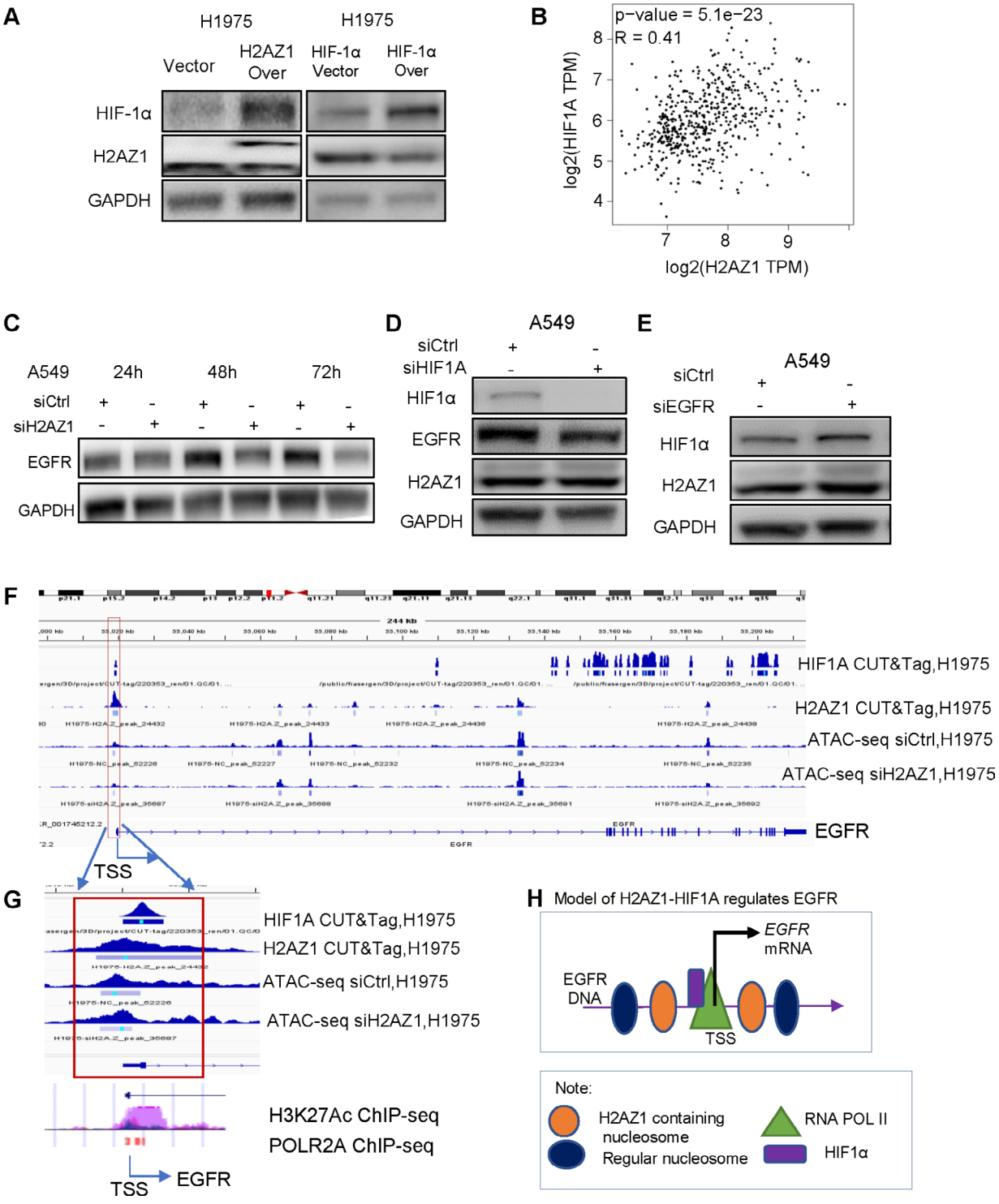

Fig. 6 H2AZ1 regulates EGFR through HIF1A. (**A**) The expression of HIF1A protein was up-regulated after H2AZ1 overexpression, while H2AZ1 protein expression was slightly down-regulated after HIF1A overexpression. (**B**) Correlation analysis on the GEPIA website suggested a strong positive correlation between *H2AZ1* mRNA and *HIF1A* mRNA ($p < 0.001$, $R = 0.41$). (**C**) EGFR protein was decreased at 24, 48, and 72 h after H2AZ1 knockdown with siRNA in the A549 cell line. (**D**) EGFR protein was downregulated after HIF1A knockdown with siRNAs, while H2AZ1 protein was not changed. (**E**) HIF1αand H2AZ1 proteins were slightly increased upon EGFR silencing with siRNA. (**F**) CUT&Tag of HIF1α indicating HIF1α protein bound to EGFR promoter and gene body regions in H1975 cell line. H2AZ1 protein was also bound to the EGFR promoter with open chromatin accessibility. (**G**) Large scale of the promoter region from **F** showing HIF1α and H2AZ1 were located at the EGFR promoter region with open chromatin accessibility for RNA polymerase binding. This region was also highly acetylated. The image of ChIP-seq of H3K27Ac and POLR2A were downloaded from the UCSC website. (**H**) Working model of H2AZ1 and HIF1α in the regulation of EGFR expression

($p<0.001$, $R=0.41$) (Fig. 6B). Our H2AZ1 CUT&Tag and ATAC-seq results showed H2AZ1 was physically bound to the TSS of HIF1A with open chromatin (ATAC-seq) for possible transcription factors and RNA polymerase binding (Fig. S6A, B). Thus, we concluded that the H2AZ1 protein binds to the TSS of the HIF1A gene, together with unknown transcription factors, to regulate HIF1A expression at the transcription level. The exact mechanism, including which transcription factors are involved, needs further investigation.

Next, we confirmed that HIF1A regulates EGFR expression. EGFR is an important oncogene in lung cancer progression and metastasis [47]. EGFR protein levels decreased after H2AZ1 knockdown in lung cancer cell lines within 24 h (Fig. 6C and S6C).

We then knocked down HIF1A with siRNAs and found that EGFR protein levels were downregulated, while H2AZ1 levels remained unchanged (Fig. 6D). HIF1αand H2AZ1 proteins were slightly upregulated after EGFR knockdown with siRNAs, whereas their mRNAs were not significantly changed (Fig. 6E and S6D). Thus, HIF1A regulated EGFR expression, while EGFR may have a slight feedback inhibitory effect on HIF1A and H2AZ1.

To uncover the physical binding region of HIF1A or H2AZ1 on EGFR, we performed CUT&Tag for HIF1A and H2AZ1. The results revealed that HIF1A and H2AZ1 were physically bound to both the promoter and gene body regions of EGFR with open chromatin (ATAC-seq) at TSS for RNA polymerase binding (Fig. 6F-H). This confirmed that HIF1A directly regulated EGFR expression at the transcription level.

Taken together, these results revealed that H2AZ1 binds to both the TSS of HIF1A and EGFR. H2AZ1 regulates EGFR expression via HIF1A's binding to the TSS of EGFR in lung cancer.

H2AZ1 regulates EGFR via the RELA-HIF1A axis

Previous studies have shown that HIF1A is regulated by RELA p65 through direct binding to the HIF1A promoter region [48, 49]. Our research demonstrated that HIF1A, RELA, and EGFR were downregulated after H2AZ1 knockdown in lung cancer cell lines. This prompted us to investigate whether H2AZ1 regulates HIF1A via RELA and subsequently affects EGFR. RELA p65 is one of the members of the transcription factor NF-κB family [41]. Analysis of existing GEPIA data indicated a strong positive correlation between RELA mRNA and HIF1A mRNA in lung adenocarcinoma tissues (Fig. 7A). To further explore the relationship between RELA and HIF1A/EGFR, we designed the siRNAs for RELA and RELB. The knockdown efficiency was validated by qRT-PCR (Fig. 7B and S7A). HIF1A mRNA and protein levels decreased after RELA knockdown (Fig. 7C, D). Notably, HIF1A expression was unaffected by RELB knockdown (Fig. S7B,). We conducted a rescue assay where RELA knockdown resulted in decreased HIF1A and EGFR levels (Fig. 7E). HIF1A and EGFR proteins were increased after HIF1A was induced by hypoxia (Fig. 7E). Furthermore, the high expression of HIF1A induced by hypoxia was able to partially rescue the decrease of EGFR caused by RELA knockdown (Fig. 7E).

To identify the physical binding region of RELA protein on the HIF1A promotor, we downloaded two RELA ChIP-seq datasets from GEO: GSE117250 [50] and GSE55105 [51]. These datasets revealed that RELA binds to the HIF1A promoter along with RNA polymerase (Fig. 7F and S7C), further confirming RELA's role in regulating HIF1A expression in lung cancer.

In our CUT&Tag and ATAC-seq results, H2AZ1 was found bound physically to the RELA promoter in regions of open chromatin (ATAC-seq) facilitating RNA polymerase binding (Fig. S7D, E). This suggests that H2AZ1 is involved in RELA expression.

In summary, the H2AZ1 protein was deposited on the TSS regions of RELA, HIF1A, and EGFR genes for their mRNA expression. H2AZ1 may regulate EGFR expression through the RELA-HIF1A axis, thereby promoting tumor progression (Fig. 7G, H).

Discussion

Although histone variant H2AZ1 plays an increasingly important role in cancer biology, the underlying mechanisms remain unclear [10]. Here, we identified the unique function and mechanisms of H2AZ1 in lung adenocarcinoma. H2AZ1 mRNA was highly expressed in lung cancer and the high level of H2AZ1 mRNA expression was associated with poor patient survival. The cell proliferation, colony formation, migration, and invasion were decreased upon H2AZ1 silence. Mechanistically, the H2AZ1 protein was predominantly deposited around TSS and influenced multiple oncogenic signaling pathways. H2AZ1 may drive lung cancer progression through the RELA-HIF1A-EGFR signaling pathway.

Our CUT&Tag-seq and RNA-seq analysis results revealed that the common H2AZ1 chromatin binding peaks among three cell lines were primarily distributed in the gene promoter region within 1 kb (77.5%), which aligns with other reports [42]. We also found that higher H2AZ1 binding intensity in the promoter region around TSS positively correlated with higher gene expression, consistent with previous reports [12, 42, 43]. Genes were expressed only when H2AZ1 was bound to the promoter (<=1 kb) and 5'UTR regions. H2AZ1 binding on chromatin could cause both upregulation and downregulation of genes upon H2AZ1 silencing.

Higher ATAC-seq peak intensity indicated that chromatin regions were more open and accessible for transcription factors and RNA polymerase binding. The

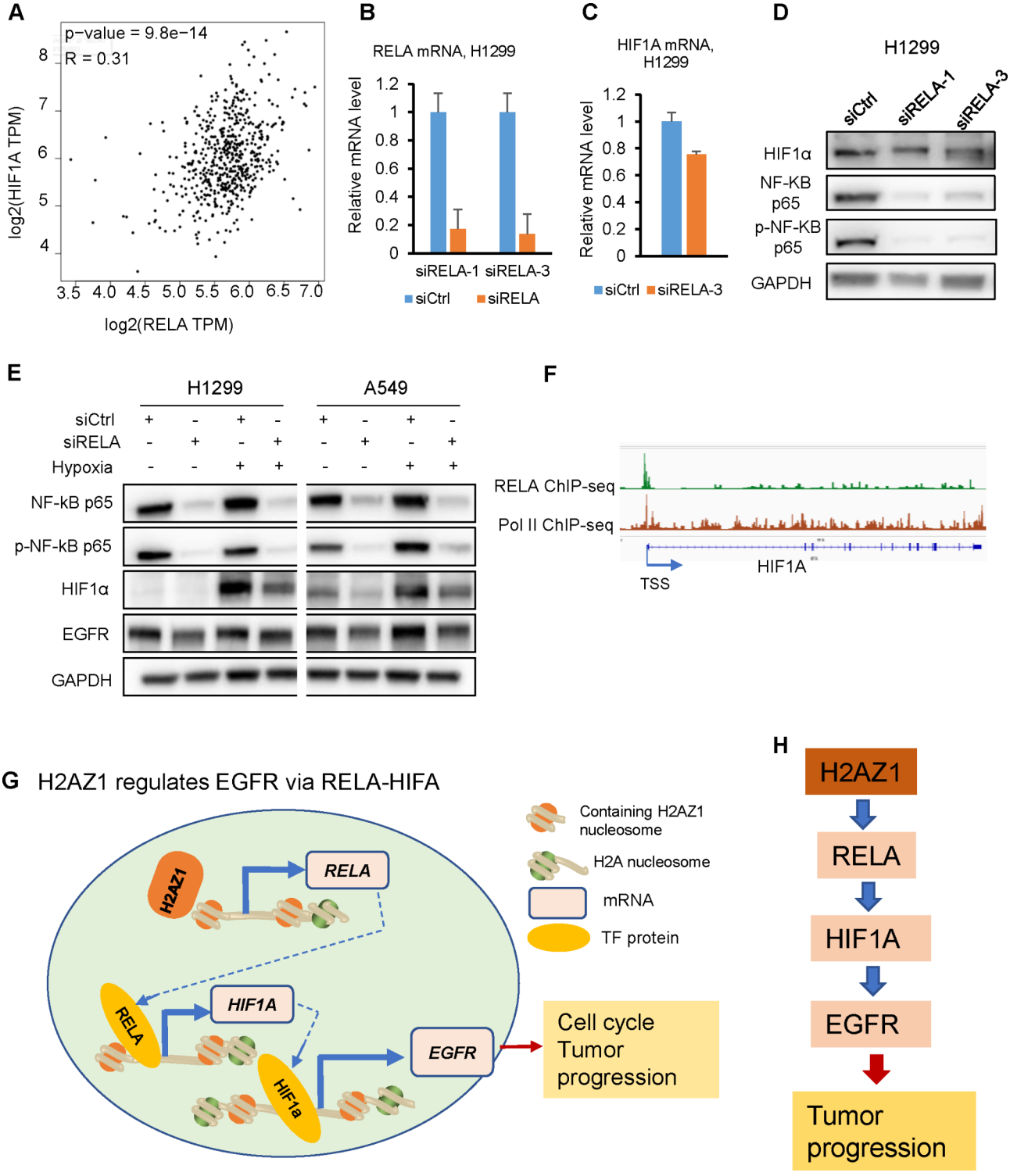

Fig. 7 H2AZ1 regulates HIF1A via RELA. (**A**) GEPIA website data indicated a strong positive correlation between RELA mRNA and HIF1A mRNA. (**B**) qRT-PCR assay validated the knockdown efficiency of RELA siRNAs in H1299 cells. (C, D) Both HIF1A mRNA and protein were decreased after RELA p65 knock-down measured by qRT-PCR and Western blot. ** $p < 0.01$. (**E**) HIF1αand EGFR proteins were decreased after RELA knockdown with siRNAs. In hypoxia status, HIF1αand EGFR proteins were increased but decreased upon RELA knockdown. (**F**) RELA protein bound to HIF1A promoter together with RNA polymerase binding measured by ChIP-seq in human B lymphoma cells. (data source: GSE117250 and GSE55105). (**G**, **H**) Working model of H2AZ1 as a central player in the RELA-HIF1A-EGFR axis

common chromatin accessibility peaks were mainly distributed in the gene promoter region within 1 kb (63%) among the three cell lines. Gene expression levels were positively correlated with higher chromatin accessibility signals only in the TSS region, and the highest gene expression levels were associated with both H2AZ1 binding and chromatin accessibility in the promoter (≤1 kb) region. Combined analyses of H2AZ1 binding from CUT&Tag-seq and gain or loss DAR region from ATAC-seq revealed a similar number of gain DAR and loss DAR in H2AZ1 binding regions, demonstrating H2AZ1 binding on chromatin could cause both gain DAR and loss DAR. These results suggested multiple factors are presented for the regulation of gene expression and chromatin accessibility other than H2AZ1 only.

H2AZ1 is reported mainly localized at promoters or enhancers [43, 52], and its chromatin deposition around TSS affects gene expression [53–56]. Our multi-omics enrichment analysis suggested that H2AZ1 regulated several key cancer-related genes/signaling pathways in lung cancer. This included several oncogenic genes such as NF-KB (RELA), MAPK, HIF1A, EGFR, CCNE1, Wnt, and Notch. We have validated some of them at protein and mRNA levels. More importantly, we revealed that H2AZ1 may regulate EGFR through RELA-HIF1A axis.

Hypoxia is a common feature of many solid tumors [57]. HIF-1 A, a hypoxia marker, governs tumor cell energy metabolism, proliferation, and apoptosis. It triggers cellular and tissue adaptations to hypoxia, promotes tumor angiogenesis, and enhances tumor invasiveness while conferring resistance to radiotherapy and chemotherapy [58]. Therefore, exploring HIF1A as an anticancer drug target has become a hot topic in recent years [59]. However, the regulation of HIF1A by the histone variant H2AZ1 has not been reported.

In this study, HIF1A was significantly downregulated upon H2AZ1 knockdown at both protein and mRNA levels. Further, HIF1A expression increased when H2AZ1 was overexpressed, while H2AZ1 expression slightly decreased after HIF1A overexpression, possibly indicating a feedback reaction. The above results confirmed that H2AZ1 regulated HIF1A at the transcription level. HIF1A is reported to be the direct target of RELA p65 through binding to the HIF1A promoter region [48, 49]. This is confirmed by another two RELA ChIP-seq datasets [50, 51], showing RELA was bound to the HIF1A promoter. We found that HIF1A was regulated by RELA at the transcription level in lung cancer cells. Thus, we speculated that H2AZ1 may regulate HIF1A through RELA.

EGFR is an important oncogene in lung cancer progression and metastasis [60, 61]. Targeting EGFR has become a key modality for lung cancer treatment. EGFR inhibitors have become first-line agents for lung cancer treatment [62]. We found that HIF1A could regulate EGFR expression and CUT&Tag results confirmed multiple HIF1A binding sites on the promoter and other regions of EGFR. Based on these results, we proposed that H2AZ1 regulates EGFR through HIF1A, and HIF1A potentially via RELA. Inhibition of H2AZ1 and its signaling may have a dual role in the treatment and prevention of lung cancer patients.

H2AZ1 was selected for this study due to its elevated expression in brain metastasis of mouse models [39], human brain metastasis of lung tumors [39, 40, 46], and various other human tumors [32, 35, 36, 63]. We performed the functional and molecular mechanistic studies in vitro, while the results of functional experiments including tumor metastasis and the related mechanisms need further exploration in vivo. The precise mechanisms by which H2AZ1 regulates RELA remain to be fully elucidated. Further experiments are needed to explore and validate this relationship. The mechanism of H2AZ1 overexpression remains poorly understood. MYC can bind to the promoter region of H2AZ1 and regulate its expression [64]. We also found that H2AZ1 expression was decreased upon MYC silencing (data not shown).

Conclusion

Histone variant H2AZ1 has an oncogenic role in lung cancer progression. H2AZ1 is mainly deposited around TSS and affects multiple cancer signaling pathways. H2AZ1 may regulate EGFR via RELA-HIF1A axis, suggesting that the intervention with H2AZ1 or its downstream genes/signaling may have translational potential for precision therapy.

Abbreviations

H2AZ1	H2A.Z Variant Histone 1
EGFR	Epidermal growth factor receptor
HIF1A	Hypoxia-inducible factor 1 alpha
RELA RELA	Proto-Oncogene, NF-KB Subunit
CUT&Tag-seq	Cleavage under targets and tagmentation with high-throughput sequencing
ATAC-seq	Assay for Transposase Accessible Chromatin with high-throughput sequencing
DAR	Differentially Accessible Region
TMA	Tissue array
TSS	Transcriptional start site

Supplementary Information

The online version contains supplementary material available at https://doi.org/10.1186/s12964-024-01823-3.

Supplementary Material 1

Acknowledgements

The authors thank Sijie Chen, Shenglin Zhang, Shengmin Hu, and Han Zhao's helpful technical assistance and discussion on this project.

Author contributions

HZ and GC designed this study and wrote the manuscript. GC supervised the study, contributed experimental data, conceptualization, and writing. HZ, XW,

YW, XL, ZZ, YL, YL and SC performed the experiments and provided helpful discussions. YD and XZ provided the help of data analysis. All authors reviewed and edited the manuscript.

Funding
This work was supported in part by the National Natural Science Foundation of China (NSFC) (32070625 to G.C.); Shenzhen Municipal Science and Technology Innovation Commission Foundation (JCYJ20210324104800001, JCYJ20220530114415036 to G.C.).

Data availability
No datasets were generated or analysed during the current study.

Declarations

Ethics approval and consent to participate
The TMA used in this study was approved by the Ethics Committee of Shanghai Outdo Biotech Company (No. YB M-05-01).

Consent for publication
Not applicable.

Competing interests
The authors declare no competing interests.

Received: 11 May 2024 / Accepted: 11 September 2024
Published online: 26 September 2024

References

1. Sung H, Ferlay J, Siegel R, Laversanne M, Soerjomataram I, Jemal A. Bray FJCacjfc: Global Cancer statistics 2020: GLOBOCAN estimates of incidence and Mortality Worldwide for 36 cancers in 185 countries. 2021, 71:209–49.
2. Siegel RL, Miller KD, Fuchs HE, Jemal A. Cancer statistics, 2022. CA Cancer J Clin. 2022;72:7–33.
3. Zheng R, Zhang S, Zeng H, Wang S, Sun K, Chen R, Li L, Wei W, He J. Cancer incidence and mortality in China, 2016. J Natl Cancer Cent. 2022;2:1–9.
4. Wang A, Wang HY, Liu Y, Zhao MC, Zhang HJ, Lu ZY, Fang YC, Chen XF, Liu GT. The prognostic value of PD-L1 expression for non-small cell lung cancer patients: a meta-analysis. Eur J Surg Oncol. 2015;41:450–6.
5. Buschbeck M, Hake SB. Variants of core histones and their roles in cell fate decisions, development and cancer. Nat Rev Mol Cell Biol. 2017;18:299–314.
6. Martire S, Banaszynski LA. The roles of histone variants in fine-tuning chromatin organization and function. Nat Rev Mol Cell Biol. 2020;21:522–41.
7. Lai S, Jia J, Cao X, Zhou PK, Gao S. Molecular and Cellular functions of the Linker histone H1.2. Front Cell Dev Biol. 2021;9:773195.
8. Das C, Tyler JK, Churchill ME. The histone shuffle: histone chaperones in an energetic dance. Trends Biochem Sci. 2010;35:476–89.
9. Sporn JC, Kustatscher G, Hothorn T, Collado M, Serrano M, Muley T, Schnabel P, Ladurner AG. Histone macroH2A isoforms predict the risk of lung cancer recurrence. Oncogene. 2009;28:3423–8.
10. Ghiraldini FG, Filipescu D, Bernstein E. Solid tumours hijack the histone variant network. Nat Rev Cancer. 2021;21:257–75.
11. Amatori S, Tavolaro S, Gambardella S, Fanelli M. The dark side of histones: genomic organization and role of oncohistones in cancer. Clin Epigenetics. 2021;13:71.
12. Vardabasso C, Gaspar-Maia A, Hasson D, Punzeler S, Valle-Garcia D, Straub T, Keilhauer EC, Strub T, Dong J, Panda T, et al. Histone variant H2A.Z.2 mediates proliferation and drug sensitivity of malignant melanoma. Mol Cell. 2015;59:75–88.
13. Bennett RL, Bele A, Small EC, Will CM, Nabet B, Oyer JA, Huang X, Ghosh RP, Grzybowski AT, Yu T, et al. A mutation in histone H2B represents a new class of oncogenic driver. Cancer Discov. 2019;9:1438–51.
14. Sales-Gil R, Kommer DC, de Castro IJ, Amin HA, Vinciotti V, Sisu C, Vagnarelli P. Non-redundant functions of H2A.Z.1 and H2A.Z.2 in chromosome segregation and cell cycle progression. EMBO Rep. 2021;22:e52061.
15. Giaimo BD, Ferrante F, Herchenröther A, Hake SB, Borggrefe T. The histone variant H2A.Z in gene regulation. Epigenetics Chromatin. 2019;12:37.
16. Corujo D, Buschbeck M. Post-translational modifications of H2A histone variants and their role in Cancer. Cancers (Basel) 2018, 10.
17. Bönisch C, Hake SB. Histone H2A variants in nucleosomes and chromatin: more or less stable? Nucleic Acids Res. 2012;40:10719–41.
18. Kalashnikova AA, Porter-Goff ME, Muthurajan UM, Luger K, Hansen JC. The role of the nucleosome acidic patch in modulating higher order chromatin structure. J R Soc Interface. 2013;10:20121022.
19. Suto RK, Clarkson MJ, Tremethick DJ, Luger K. Crystal structure of a nucleosome core particle containing the variant histone H2A.Z. Nat Struct Biol. 2000;7:1121–4.
20. Giaimo BD, Ferrante F, Vallejo DM, Hein K, Gutierrez-Perez I, Nist A, Stiewe T, Mittler G, Herold S, Zimmermann T, et al. Histone variant H2A.Z deposition and acetylation directs the canonical notch signaling response. Nucleic Acids Res. 2018;46:8197–215.
21. Marques M, Laflamme L, Gervais AL, Gaudreau L. Reconciling the positive and negative roles of histone H2A.Z in gene transcription. Epigenetics. 2010;5:267–72.
22. Talbert PB, Henikoff S. Histone variants–ancient wrap artists of the epigenome. Nat Rev Mol Cell Biol. 2010;11:264–75.
23. Hua S, Kallen CB, Dhar R, Baquero MT, Mason CE, Russell BA, Shah PK, Liu J, Khramtsov A, Tretiakova MS, et al. Genomic analysis of estrogen cascade reveals histone variant H2A.Z associated with breast cancer progression. Mol Syst Biol. 2008;4:188.
24. Brunelle M, Nordell Markovits A, Rodrigue S, Lupien M, Jacques P, Gévry N. The histone variant H2A.Z is an important regulator of enhancer activity. Nucleic Acids Res. 2015;43:9742–56.
25. Valdes-Mora F, Song JZ, Statham AL, Strbenac D, Robinson MD, Nair SS, Patterson KI, Tremethick DJ, Stirzaker C, Clark SJ. Acetylation of H2A.Z is a key epigenetic modification associated with gene deregulation and epigenetic remodeling in cancer. Genome Res. 2012;22:307–21.
26. Hsu CC, Shi J, Yuan C, Zhao D, Jiang S, Lyu J, Wang X, Li H, Wen H, Li W, Shi X. Recognition of histone acetylation by the GAS41 YEATS domain promotes H2A.Z deposition in non-small cell lung cancer. Genes Dev. 2018;32:58–69.
27. Zheng Y, Han X, Wang T. Role of H2A.Z.1 in epithelial-mesenchymal transition and radiation resistance of lung adenocarcinoma in vitro. Biochem Biophys Res Commun. 2022;611:118–25.
28. Corces MR, Trevino AE, Hamilton EG, Greenside PG, Sinnott-Armstrong NA, Vesuna S, Satpathy AT, Rubin AJ, Montine KS, Wu B. An improved ATAC-seq protocol reduces background and enables interrogation of frozen tissues. Nat Methods. 2017;14:959–62.
29. Fujiwara S, Baek S, Varticovski L, Kim S, Hager GL. High quality ATAC-Seq data recovered from cryopreserved breast cell lines and tissue. Sci Rep. 2019;9:1–11.
30. Kaya-Okur HS, Wu SJ, Codomo CA, Pledger ES, Bryson TD, Henikoff JG, Ahmad K, Henikoff S. CUT&Tag for efficient epigenomic profiling of small samples and single cells. *Nat Commun* 2019, 10:1930.
31. Okayama H, Kohno T, Ishii Y, Shimada Y, Shiraishi K, Iwakawa R, Furuta K, Tsuta K, Shibata T, Yamamoto S, et al. Identification of genes upregulated in ALK-positive and EGFR/KRAS/ALK-negative lung adenocarcinomas. Cancer Res. 2012;72:100–11.
32. Shedden K, Taylor J, Enkemann S, Tsao M, Yeatman T, Gerald W, Eschrich S, Jurisica I, Giordano T, Misek D et al. Gene expression-based survival prediction in lung adenocarcinoma: a multi-site, blinded validation study. 2008, 14:822–7.
33. Hou J, Aerts J, den Hamer B, van Ijcken W, den Bakker M, Riegman P, van der Leest C, van der Spek P, Foekens JA, Hoogsteden HC, et al. Gene expression-based classification of non-small cell lung carcinomas and survival prediction. PLoS ONE. 2010;5:e10312.
34. Irizarry RA, Hobbs B, Collin F, Beazer-Barclay YD, Antonellis KJ, Scherf U, Speed TP. Exploration, normalization, and summaries of high density oligonucleotide array probe level data. Biostatistics. 2003;4:249–64.
35. Seo JS, Ju YS, Lee WC, Shin JY, Lee JK, Bleazard T, Lee J, Jung YJ, Kim JO, Shin JY, et al. The transcriptional landscape and mutational profile of lung adenocarcinoma. Genome Res. 2012;22:2109–19.
36. Cancer Genome Atlas Research N. Comprehensive molecular profiling of lung adenocarcinoma. Nature. 2014;511:543–50.
37. Trapnell C, Williams BA, Pertea G, Mortazavi A, Kwan G, van Baren MJ, Salzberg SL, Wold BJ, Pachter L. Transcript assembly and quantification by RNA-Seq reveals unannotated transcripts and isoform switching during cell differentiation. Nat Biotechnol. 2010;28:511–5.
38. Robinson JT, Thorvaldsdottir H, Winckler W, Guttman M, Lander ES, Getz G, Mesirov JP. Integrative genomics viewer. Nat Biotechnol. 2011;29:24–6.

39. Boire A, Zou Y, Shieh J, Macalinao DG, Pentsova E, Massague J. Complement component 3 adapts the Cerebrospinal Fluid for Leptomeningeal Metastasis. Cell. 2017;168:1101–e11131113.
40. Kikuchi T, Daigo Y, Ishikawa N, Katagiri T, Tsunoda T, Yoshida S, Nakamura Y. Expression profiles of metastatic brain tumor from lung adenocarcinomas on cDNA microarray. Int J Oncol. 2006;28:799–805.
41. Tang Z, Li C, Kang B, Gao G, Li C, Zhang Z. GEPIA: a web server for cancer and normal gene expression profiling and interactive analyses. Nucleic Acids Res. 2017;45:W98–102.
42. Barski A, Cuddapah S, Cui K, Roh TY, Schones DE, Wang Z, Wei G, Chepelev I, Zhao K. High-resolution profiling of histone methylations in the human genome. Cell. 2007;129:823–37.
43. Hu G, Cui K, Northrup D, Liu C, Wang C, Tang Q, Ge K, Levens D, Crane-Robinson C, Zhao K. H2A.Z facilitates access of active and repressive complexes to chromatin in embryonic stem cell self-renewal and differentiation. Cell Stem Cell. 2013;12:180–92.
44. Sherman BT, Hao M, Qiu J, Jiao X, Baseler MW, Lane HC, Imamichi T, Chang W. DAVID: a web server for functional enrichment analysis and functional annotation of gene lists (2021 update). Nucleic Acids Res 2022.
45. Gillette MA, Satpathy S, Cao S, Dhanasekaran SM, Vasaikar SV, Krug K, Petralia F, Li Y, Liang WW, Reva B, et al. Proteogenomic characterization reveals therapeutic vulnerabilities in Lung Adenocarcinoma. Cell. 2020;182:200–e225235.
46. Mamo M, Ye IC, DiGiacomo JW, Park JY, Downs B, Gilkes DM. Hypoxia alters the response to Anti-EGFR therapy by regulating EGFR expression and downstream signaling in a DNA methylation-specific and HIF-Dependent manner. Cancer Res. 2020;80:4998–5010.
47. Noronha A, Belugali Nataraj N, Sang Lee J, Zhitomirsky B, Oren Y, Oster S, Lindzen M, Mukherjee S, Will R, Ghosh S et al. AXL and error-prone DNA replication confer drug resistance and offer strategies to treat EGFR-mutant lung cancer. Cancer Discov 2022.
48. Rius J, Guma M, Schachtrup C, Akassoglou K, Zinkernagel AS, Nizet V, Johnson RS, Haddad GG, Karin M. NF-kappaB links innate immunity to the hypoxic response through transcriptional regulation of HIF-1alpha. Nature. 2008;453:807–11.
49. Li ZL, Ji JL, Wen Y, Cao JY, Kharbuja N, Ni WJ, Yin D, Feng ST, Liu H, Lv LL, et al. HIF-1alpha is transcriptionally regulated by NF-kappaB in acute kidney injury. Am J Physiol Ren Physiol. 2021;321:F225–35.
50. Zhao M, Joy J, Zhou W, De S, Wood WH 3rd, Becker KG, Ji H, Sen R. Transcriptional outcomes and kinetic patterning of gene expression in response to NF-kappaB activation. PLoS Biol. 2018;16:e2006347.
51. Zhao B, Barrera LA, Ersing I, Willox B, Schmidt SC, Greenfeld H, Zhou H, Mollo SB, Shi TT, Takasaki K, et al. The NF-kappaB genomic landscape in lymphoblastoid B cells. Cell Rep. 2014;8:1595–606.
52. Colino-Sanguino Y, Clark SJ, Valdes-Mora F. The H2A.Z-nuclesome code in mammals: emerging functions. Trends Genet. 2022;38:273–89.
53. Bargaje R, Alam MP, Patowary A, Sarkar M, Ali T, Gupta S, Garg M, Singh M, Purkanti R, Scaria V, et al. Proximity of H2A.Z containing nucleosome to the transcription start site influences gene expression levels in the mammalian liver and brain. Nucleic Acids Res. 2012;40:8965–78.
54. Cole L, Kurscheid S, Nekrasov M, Domaschenz R, Vera DL, Dennis JH, Tremethick DJ. Multiple roles of H2A.Z in regulating promoter chromatin architecture in human cells. Nat Commun. 2021;12:2524.
55. Liu X, Zhang J, Zhou J, Bu G, Zhu W, He H, Sun Q, Yu Z, Xiong W, Wang L et al. Hierarchical Accumulation of histone variant H2A.Z regulates Transcriptional States and histone modifications in early mammalian embryos. Adv Sci (Weinh) 2022:e2200057.
56. Murphy KE, Meng FW, Makowski CE, Murphy PJ. Genome-wide chromatin accessibility is restricted by ANP32E. Nat Commun. 2020;11:5063.
57. Muz B, de la Puente P, Azab F, Azab AK. The role of hypoxia in cancer progression, angiogenesis, metastasis, and resistance to therapy. Hypoxia (Auckl). 2015;3:83–92.
58. Masoud GN, Li W. HIF-1α pathway: role, regulation and intervention for cancer therapy. Acta Pharm Sin B. 2015;5:378–89.
59. Soni S, Padwad YS. HIF-1 in cancer therapy: two decade long story of a transcription factor. Acta Oncol. 2017;56:503–15.
60. da Cunha Santos G, Shepherd FA, Tsao MS. EGFR mutations and lung cancer. Annu Rev Pathol. 2011;6:49–69.
61. Levin PA, Brekken RA, Byers LA, Heymach JV, Gerber DE. Axl receptor Axis: a New Therapeutic Target in Lung Cancer. J Thorac Oncol. 2016;11:1357–62.
62. Ettinger DS, Wood DE, Aisner DL, Akerley W, Bauman JR, Bharat A, Bruno DS, Chang JY, Chirieac LR, D'Amico TA, et al. Non-small Cell Lung Cancer, Version 3.2022, NCCN Clinical Practice guidelines in Oncology. J Natl Compr Canc Netw. 2022;20:497–530.
63. Hou J, Aerts J, den Hamer B, van Ijcken W, den Bakker M, Riegman P, van der Leest C, van der Spek P, Foekens J, Hoogsteden H et al. Gene expression-based classification of non-small cell lung carcinomas and survival prediction. 2010, 5:e10312.
64. Magri L, Gacias M, Wu M, Swiss VA, Janssen WG, Casaccia P. c-Myc-dependent transcriptional regulation of cell cycle and nucleosomal histones during oligodendrocyte differentiation. Neuroscience. 2014;276:72–86.

Publisher's note